



HAL
open science

Integrated approach for the processing of a complex tungsten Skarn ore (Tabuaço, Portugal)

Y. Foucaud, I. Filippova, Q. Dehaine, P. Hubert, L. Filippov

► **To cite this version:**

Y. Foucaud, I. Filippova, Q. Dehaine, P. Hubert, L. Filippov. Integrated approach for the processing of a complex tungsten Skarn ore (Tabuaço, Portugal). *Minerals Engineering*, 2019, 143, pp.105896. 10.1016/j.mineng.2019.105896 . hal-03487286

HAL Id: hal-03487286

<https://hal.science/hal-03487286v1>

Submitted on 20 Jul 2022

HAL is a multi-disciplinary open access archive for the deposit and dissemination of scientific research documents, whether they are published or not. The documents may come from teaching and research institutions in France or abroad, or from public or private research centers.

L'archive ouverte pluridisciplinaire **HAL**, est destinée au dépôt et à la diffusion de documents scientifiques de niveau recherche, publiés ou non, émanant des établissements d'enseignement et de recherche français ou étrangers, des laboratoires publics ou privés.



Distributed under a Creative Commons Attribution - NonCommercial 4.0 International License

Integrated Approach for the Processing of a Complex Tungsten Skarn Ore (Tabuaço, Portugal)

Y. Foucaud¹, I. Filippova^{1,2}, Q. Dehaine^{3,4}, P. Hubert¹, L. Filippov^{1,2}

¹Université de Lorraine, CNRS, GeoRessources laboratory, F-54000 Nancy, France

²National University of science and technology MISIS, 119049 Moscow, Russia

³University of Exeter, Camborne School of Mines, Penryn, Cornwall, TR10 9FE, United Kingdom

⁴Geological Survey of Finland, P.O. Box 96, F1-02151, Espoo, Finland

Abstract

The Tabuaço tungsten project, located in Northern Portugal, consists of two skarn layers, namely “Main” and “Lower” skarns, which display significantly different mineralogical and geochemical features. Both skarns contain fine-grained disseminated scheelite, but the Lower-skarn gangue is dominated by silicates whereas the Main-skarn gangue contains calcium-bearing minerals including fluorite, apatite, and vesuvianite, in close association with scheelite. Preliminary feasibility studies showed that direct separation of calcium-bearing minerals by flotation with fatty acids, which are environmentally benign, was unsuccessful due to their similar surface properties. Several routes for each skarn type were proposed with a strong focus on the Main skarn that displays the most complex mineralogical associations. Enhanced gravity separation (Falcon concentrator), high intensity magnetic separation, and flotation with fatty acids were investigated for the Main Skarn level with the objective of producing a marketable scheelite concentrate. Flotation was thoroughly investigated in terms of depressants, producing optimally a concentrate assaying 9.2% WO₃ at 87.9% WO₃ recovery from a ~1.1% WO₃ feed, by means of a 1:1 ratio of sodium carbonate and sodium silicate. Fluorite is the most problematic mineral in flotation with fatty acids and, consequently, new fatty-acids-based collector formulations have been developed to improve the separation contrast between scheelite and fluorite, producing a concentrate assaying 14.1% WO₃ with 77.1% WO₃ recovery for the fully-optimised conditions. Furthermore, the performance of two types of Falcon bowls (SB and UF) were investigated and optimised for gangue

minerals rejection. The Falcon concentrator was used as a desliming and pre-concentrating apparatus: one stage of Falcon SB allowed rejection of 84% of the total amount of fluorite, more than 95% of the slimes, and 85 wt.% of the mass. Consequently, it improved significantly the performance of the fully-optimised scheelite flotation as the final concentrate, after one Falcon SB stage and 4 flotation stages, assayed 62.9% WO₃ with 59.4% WO₃ recovery, which constituted a marketable scheelite concentrate. Both the Falcon SB parameters and the number of fully-optimised flotation stages can be optimised to maximise either the WO₃ grade or the WO₃ recovery, regarding the product specifications. Finally, the high intensity magnetic separation allowed rejection of around 45 wt.% of the total yield prior to the milling stage with only 6.0% WO₃ losses, which would decrease significantly the energy consumed during the milling stage.

1. Introduction

Tungsten has gathered considerable interest in the European Union over the past few years due to its high economic importance, low recycling rate and few substitution possibilities (Audion and Labbé, 2012; European Commission, 2010). In addition, tungsten is subject to high supply risks, mainly attributed to the control of China over the global tungsten supply market (Pitfield et al., 2011). Currently, due to the low recycling rate, primary tungsten is still the major source of tungsten for the production of manufactured products such as alloys, supra-alloys, and tungsten carbide (Audion and Labbé, 2012; Pitfield et al., 2011). Scheelite (CaWO₄) and wolframite [(Fe,Mn)WO₄] are the two main minerals exploited for primary tungsten extraction. Wolframite is usually processed by classical gravity, magnetic, and occasionally froth flotation methods, due to high liberation mesh and simple quartz-based gangues. Scheelite is mostly encountered in skarn deposits, which represent more than 40% of the global current tungsten reserves (Pitfield et al., 2011), and is mainly processed by flotation although a gravity separation can be suitable. Since the tungsten price has significantly increased over the last decade, tungsten skarn deposits have drawn significant worldwide attention, despite their moderate complexity.

1.1. The Tabuaço deposit: a middle-sized world-class tungsten skarn

The Tabuaço tungsten deposit is located in Northern Portugal, at the north of the Central Iberian zone of the Iberian Massif that is part of the Variscan belt (Fig. 1a). As with many other scheelite-skarn occurrences, the Tabuaço deposit is hosted in Cambrian metasediments, at the northern margin of Variscan granitoids such as the Paredes da Beira-Tabuaço (PBT) granite (Dias et al., 2014; Foucaud et al., 2018b; Pinto et al., 2016), see Fig. 1b. It comprises two sub-deposits called Aveleira and São Pedro das Águas. The present study concerns the latter, which accounts for 71% of the global Tabuaço deposit resources. São Pedro das Águas sub-deposit consists in a ~100 m thick layer of metasedimentary rocks in which two mineralised zones are included (Fig. 1c). A NI 43-101, published in 2011, indicated and inferred resource of 2 Mt. with a 0.56% WO_3 average grade ranking Tabuaço as a middle-sized world-class tungsten deposit (Dawson, 1995). The two mineralised layers, called “Lower Skarn” and “Main Skarn”, are sub-parallel to the contact between the PBT granite and the Bateiras Formation, which exhibits numerous others lower-sized scheelite-skarns occurrences (Fig. 1).

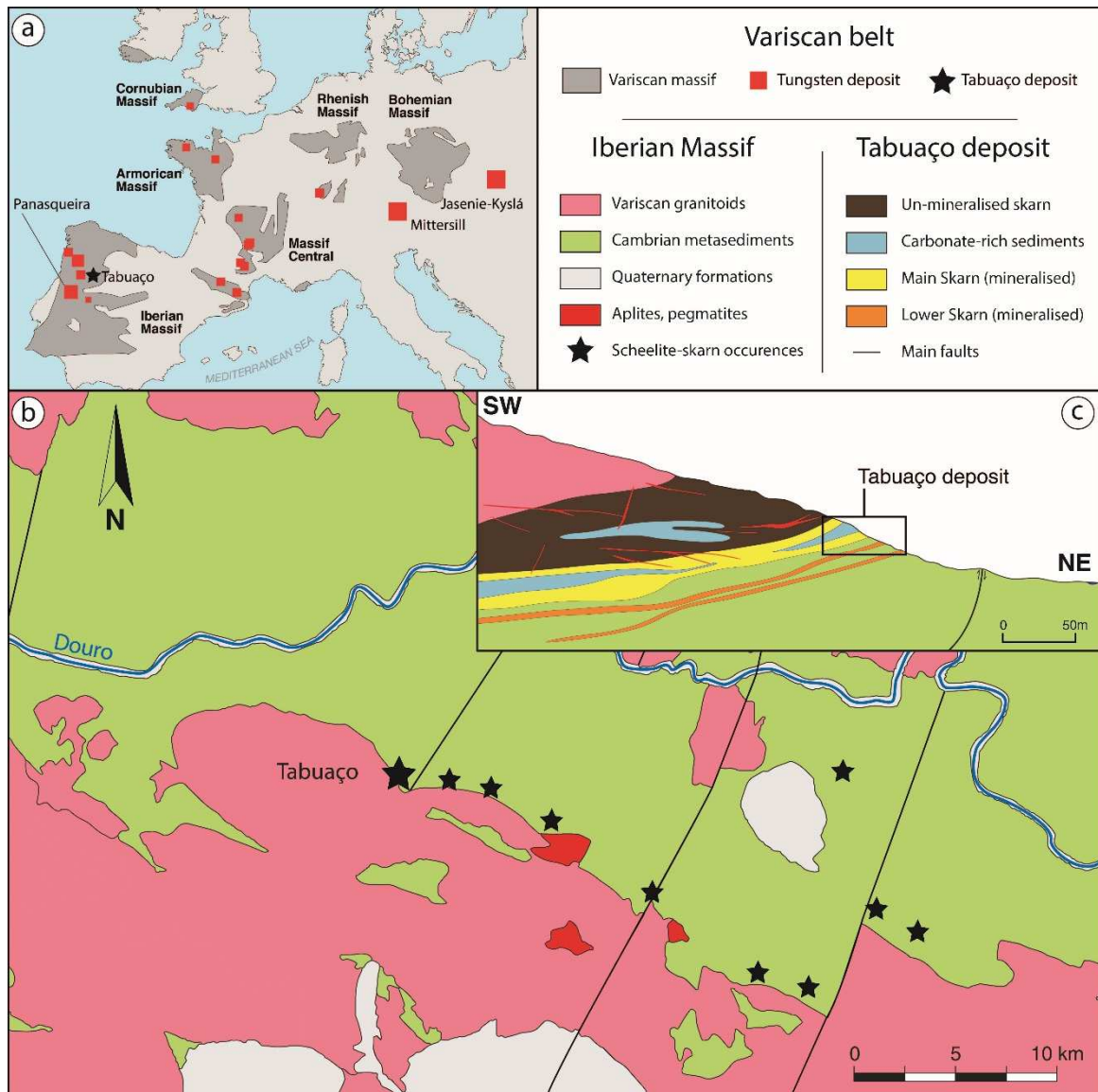


Fig. 1. (a) Location of the Tabuaço deposit and other European tungsten deposits associated with the Variscan belt, modified after (Dehaine et al., 2019a); (b) structural map of the Tabuaço deposit and associated scheelite-skarns occurrences, modified after (Foucaud et al., 2018b); (c) SW-NE cross section of the Tabuaço deposit, modified after (Foucaud et al., 2018b).

1.2. Skarn ores processing options

In skarn ores, scheelite is commonly finely disseminated and associated with calcium-bearing minerals such as calcite, dolomite, fluorite, and apatite (Jébrak et al., 2016; Kupka and Rudolph, 2018; Yang, 2018). The fine liberation **size** makes it difficult to process these ores by classical gravity separation methods, *e.g.* shaking tables, jigs, or spirals (Blazy and Joussemet, 2011; Das and Sarkar, 2018; Wells, 1991). The froth flotation technique **is preferred** since it enables the beneficiation of fine-grained ores, down to 10 µm, with relatively high throughputs.

Nowadays, few routes exist for efficient industrial-scale scheelite flotation (Kupka and Rudolph, 2018; Yang, 2018). Amine collectors demonstrated acceptable performances although they are known to float silicates due to their physisorption on negatively-charged surfaces (Arnold et al., 1978; Hiçyılmaz et al., 1993). Since silicates represent 85%-95% of the Tabuaço ore, the use of amines seems unsuited to attain a good selectivity. Another method consists **of** the **utilisation** of hydroxamic acids, **mainly** benzohydroxamic acid, often in combination with lead cations (Deng et al., 2016; Feng et al., 2017; Kupka and Rudolph, 2018; Zhao et al., 2015, 2013). In the European Union, benzene-based compounds are forbidden and the industrial use of lead is strictly restricted, making this method impossible to apply for the Tabuaço deposit. The last proofed and widely used route is the flotation with fatty acids as collectors, especially sodium oleate, which are very efficient, cheap, and environmental-friendly (Agar, 1984; Bo et al., 2015a; Miller and Misra, 1984; Pugh and Stenius, 1985; Rao et al., 1988; Yongxin and Changgen, 1983a). At industrial-scale, Tall Oil Fatty Acids (TOFA), a by-product of the Kraft wood process, are mostly used, making the flotation collectors even cheaper. Their high efficiency is attributed to the chemisorption of the carboxylate group onto surface calcium atoms (Atademir et al., 1979; Filippova et al., 2014; Foucaud et al., 2018a; K. I. Marinakis and Shergold, 1985). However, the two **mineralised** layers of Tabuaço deposit, particularly the Main Skarn, display high amounts of calcium-bearing minerals, either **calcium silicates** or **calcium** semi-soluble salts (fluorite, apatite, calcite, and scheelite). Hence, flotation separation of calcium minerals with fatty acids is difficult since they chemisorb onto the surface calcium atoms, inducing a **non-selective** flotation (Atademir et al., 1979; Filippova et al., 2014; Foucaud et al., 2018a; K. I. Marinakis and Shergold, 1985). Different solutions

can be undertaken to improve the elimination of calcium-bearing minerals during the mineral processing stage. Depressants can be added in flotation to enhance the separation **differential** between scheelite and the troublemaking minerals (Abeidu, 1973; Bo et al., 2015b; Chen et al., 2017; Gao et al., 2015; Kupka and Rudolph, 2018; Liu et al., 2016, 2017; K.I. Marinakis and Shergold, 1985; Wang and Yu, 2007; Yongxin and Changgen, 1983b; Zhang et al., 2017). Nevertheless, **although** silicates are quite easily depressed, very few depressants are selective between scheelite and fluorite, apatite, and calcite. According to recent developments, the flotation selectivity regarding the above-mentioned gangue minerals can be enhanced using mixtures of fatty acids with different aliphatic chain structures (Filippov et al., 2018).

Additionally, the minerals commonly contained in tungsten skarns, including the Tabuaço skarn, exhibit a large range of specific gravities: 2.7 for calcite, 3.2 for fluorite and apatite, and 6.1 for scheelite while silicates have specific gravities between 2.6 and 3.7, depending on the geological **context. Hence,** it **allows one** to perform a gravity separation to eliminate the minerals that are problematic in flotation with fatty acids, mostly the calcium-bearing semi-soluble salts (calcite, apatite, and fluorite). Nevertheless, the frequent fine liberation **size** make difficult the use of classical gravity separation methods as shaking tables, spirals, or jigs. For **a** few decades, the ores have exhibited finer and finer liberations **sizes** leading to a significant decrease of the efficiency of classical gravity separation methods. **It introduced** the development of special devices **such** as Multi-Gravity Separators (MGS), Knelson concentrator, and Falcon concentrator to achieve efficient density separation of fine particles (Blazy and Joussemet, 2011). Such methods can be operated on ultrafine particles, down to 3 µm (Blazy and Joussemet, 2011; Das and Sarkar, 2018; Falconer, 2003) and thus can be efficient on skarn ores **such as** the Tabuaço ore. However, due to the relatively low enrichment ratios obtained with such devices compared to flotation, they are often combined with additional upgrading steps of used for feed preparation prior to flotation (Filippov et al., 2016).

Also, skarns commonly **contain** iron that is **found within** the ferromagnesian silicates of the protolith. After the thermometamorphism stage, iron is often included in the newly-formed dense silicates such as vesuvianite, epidote, and garnets. Due to the iron they contain, these silicates, which are denser

compared to the non-ferromagnesian silicates, exhibit significant magnetic susceptibility, ranking them in the paramagnetic minerals class. Hence, a high intensity magnetic separation is possible to eliminate these minerals that can represent high amounts in the skarns, including the Tabuaço skarn.

The gangue calcium-bearing minerals often comprise elements such as P, Si, C, and F that are considered (along with sulphur) as penalizing elements either for the scheelite concentrates processed by hydrometallurgy or for the final metal-tungsten product (Pastor, 2000; Pitfield et al., 2011; Yang et al., 2016). Moreover, the lack of selectivity leads to a dilution of scheelite in the concentrates **in** which WO_3 grades are not high enough for the hydrometallurgy process that requires $>60\%$ WO_3 concentrates (Pastor, 2000; Pitfield et al., 2011). Hence, removal of fluorite, apatite, calcite, and calcium-bearing silicates prior to any hydrometallurgical treatment is of paramount interest.

This study presents an integrated approach undertaken on a fine-grained tungsten skarn ore from the Tabuaço deposit, which contains scheelite in association with fluorite, apatite, calcite, and calcium-bearing silicates. The deposit and ore characteristics are discussed, focussing particularly on their implications to develop an efficient and environmentally friendly process. Several individual options suggested hereby were tested and optimised in previous studies and have been repeated for this study. Taking also into account the product specifications for the scheelite concentrates and the previous results, different flowsheets combining the optimised separations are investigated to process the ore. The different routes are compared in terms of performances, operating costs, and environmental friendliness.

2. Materials and methods

2.1. Materials and sample preparation

A trenching sampling campaign allowed two bulk samples of 500 kg **to be acquired from** each of the two **mineralised** layers for metallurgical testing. These samples were firstly used to characterise the Tabuaço ore in terms of geochemistry, mineralogy, and textures.

The bulk samples were crushed in successive jaw crushing steps and, finally, in a gyratory crusher to produce a -4 mm material. This product was wet sieved at 150 µm and the non-passing fraction was ground in a steel laboratory ball mill to reach the liberation mesh. The ground ore was deslimed at 10 µm by means of a 50 mm hydrocyclone prior to flotation and wet magnetic separation testing.

2.2. Chemical analyses

All the products were analysed by Energy Dispersive X-Ray fluorescence spectroscopy (ED-XRF) using a Niton™ XL3t (Thermo Scientific) portable analyser. Results were corrected by external calibration using standards analysed by ICP-AES/ICP-MS at the *Service d'Analyses des Roches et des Minéraux* (SARM-CNRS, Nancy, France). The fluorine content was estimated by a multivariate calibration determined with 100 standards analysed by potentiometric measurements at the SARM-CNRS. The WO₃, P₂O₅, and F recoveries were calculated and used to assess the separation performances in terms of scheelite, apatite, and fluorite, respectively. Additionally, the K₂O recovery was used as a proxy to estimate the separation performance in terms of light silicates, which are dominated by potassium feldspars and display similar properties. Finally, the Fe₂O₃ recovery was used to assess the separation performance for the dense silicates since the total iron of the ore is divided into all the dense silicates which also exhibit similar properties.

2.3. Optical microscopic analyses

The metallurgical testing performances were also assessed by optical microscopy, using a Nikon OptiPhot-2, which supplemented the chemical analyses and allowed the results to be evaluated in terms of mineralogy. After the tests, the products were dried and representative aliquots of around 10 g were put in resin to make a 30-µm-thick thin section. Both polarised and cross-polarised lights were used to identify the minerals.

2.4. Magnetic separation

High intensity magnetic separation tests were performed in both dry and wet conditions. In dry conditions, the tests were conducted using a PermRoll® magnetic separator equipped with a neodymium-

iron-boron permanent magnet (≈ 1 T) on the $-500+150$ μm fraction, corresponding to the crushed product prior to fine grinding. The angle of the separation flap and the feed belt speed were adjusted to maximise scheelite recovery. Wet magnetic separation was performed on the flotation feed, namely, the $-150+10$ μm product, with a plate type JONES[®] magnetic separator, operated with an electromagnetic induction of 1 T. The middlings were mixed with the non-magnetic fraction to maximise the scheelite recovery.

2.5. Falcon

The Falcon tests were performed using a Falcon L40 laboratory model (Sepro Mineral Systems, Canada) equipped with a 4" smooth-walled Falcon UF bowl or fluidised Falcon SB bowl. The feed was kept constant in terms of sizes and densities using an adapted mixer, fed with a peristaltic pump to ensure a constant flowrate. Falcon tests were conducted on the $-150+0$ μm product with optimised operating parameters as defined in a previous study (Foucaud et al., 2019a). All the Falcon tests were performed at 2 wt.% solids in the pulp feeding the apparatus with a $3 \text{ kg}\cdot\text{min}^{-1}$ pulp flowrate. The rotary speed was set to 70 Hz for the Falcon UF and to 58 Hz for the Falcon SB. For the latter, the fluidisation pressure was set to 3 PSI. Feed dry weight was set at 500 g based on preliminary saturation tests to set the maximum feed weight to avoid saturation of the bowl (Dehaine et al., 2019b).

2.6. Flotation

2.6.1. Reagents

Two different commercial Tall Oil Fatty Acids (TOFA) were used as collectors for the flotation tests. The first TOFA was RBD15 (MeadWestvaco), composed of oleic acid (36 wt.%), linoleic acid (25 wt.%), and negligible amounts of palmitic and linolenic acids. The second collector, named LD, was roughly the same but with a significantly higher quantity of saturated fatty acids, namely palmitic and stearic acids. The mixture was prepared in aqueous conditions at alkaline pH, obtained via the addition of sodium hydroxide. The pH modifiers (NaOH and Na_2CO_3) and the depressant (Na_2SiO_3) used, of technical quality, were supplied by Sigma Aldrich.

2.6.2. Flotation tests

Laboratory scale flotation tests were performed using an Agitair LA-500 rotor-apparatus equipped with a 1.5 L cell in which the rotational speed was set at 900 rpm during conditioning and flotation. The cell was fed with 500 g of the -150+10 μm material which were conditioned in the cell with tap water at pH 10-10.5 for 1 min, with the depressant for 5 min, and with the collector for 3 min. The pH was adjusted to 10-10.5 by the addition of NaOH. The tests were conducted at room temperature, with a solid-liquid ratio of 33 wt.%. During the flotation tests, the airflow was set at 0.27 $\text{m}^3\cdot\text{h}^{-1}$ and the froth was recovered every 2 s for 3 min.

3. Results

3.1. Ore characterisation

The ore types present in the Tabuaço deposit were significantly different in terms of geochemistry, mineralogical association, and tungsten average grade (Table 1). The Lower Skarn displayed higher SiO_2 and Fe_2O_3 contents, while the Main Skarn exhibited higher CaO, F, P_2O_5 , and W contents. It could be related to their distance to the granite intrusion since the Lower Skarn was further away from the granite than the Main Skarn (Fig. 1c). It could also be attributed to significant differences in the protoliths chemistry: the Lower Skarn derived from a more-siliceous rock while the Main Skarn from a more-calcareous rock (Table 1).

The Main Skarn was composed of silicates (85 wt.%), mostly calcium-bearing silicates (vesuvianite, zoisite, and grossular) and, to a lesser extent, feldspars and quartz (Table 1; Fig. 2b, c, d). The remaining fraction comprised fluorite, apatite, and scheelite. It presented massive coarse-grained textures with grain sizes varying from few micrometres to more than 1 cm. Scheelite was often finely disseminated and rarely laminated, overprinting sedimentary structures. It formed 5 to 300 μm anhedral crystals with an average size of 150 μm , which constituted the liberation size for the Main Skarn. Very close mineral associations were exhibited between scheelite and fluorite/vesuvianite with a significant proportion of intergrowth crystals (Foucaud et al., 2018b). Moreover, pervasive albitisation of the skarn horizons,

principally the Main Skarn, affected the whole paragenesis including scheelite and could induce significant proportions of intergrowth crystals (Foucaud et al., 2018b).

Table 1. Summary of the main geological, geochemical, and mineralogical characteristics of the Main and Lower skarns.

Characteristics	Main Skarn	Lower Skarn
<i>Geological</i>		
Mineralisation	Disseminated scheelite	Disseminated scheelite
Protolithic geochemistry	Laminated scheelite CaO>SiO ₂	CaO<SiO ₂
Average scheelite grain size	180 µm	120 µm
<i>Geochemical</i>		
	wt.%	wt.%
WO ₃	1.13	0.28
SiO ₂	41.17	47.25
Al ₂ O ₃	17.83	17.14
Fe ₂ O ₃	2.41	6.06
MgO	1.82	2.31
CaO	27.28	21.38
Na ₂ O	1.72	1.86
K ₂ O	1.11	0.94
P ₂ O ₅	1.05	0.33
F	4.05	1.47
<i>Mineralogical</i>		
	wt.%	wt.%
Vesuvianite	Ca ₁₀ (Mg,Fe) ₂ Al ₄ (SiO ₄) ₅ (Si ₂ O ₇) ₂ (OH) ₄	40-65
Feldspars	(Na,K)AlSi ₃ O ₈	15-20
<u>Fluorite</u>	CaF ₂	1-3
Zoisite	Ca ₂ (Al,Fe) ₃ (SiO ₄) ₃ (OH)	15-25
Grossular	Ca ₃ (Al,Fe) ₂ (SiO ₄) ₃	5
Clay minerals	N/A	5
<u>Fluorapatite</u>	Ca ₅ (PO ₄) ₃ F	3
Quartz	SiO ₂	10-20
<u>Scheelite</u>	CaWO ₄	0.50
<u>Calcite</u>	CaCO ₃	2

The Lower Skarn contained mostly silicates (95 wt.%) including significant amounts of vesuvianite, diopside, zoisite, quartz, and feldspars. This layer was poor in calcium-bearing salts, exhibiting low levels of fluorite, apatite, and scheelite. However, higher contents of calcite were exhibited in this facies as well as a few sulphides, mainly arsenopyrite, pyrite, and pyrrhotite, which were not identified in the Main Skarn level. It also displayed finer textures and, thus, finer scheelite liberation size, estimated at around 100-120 µm by optical microscopy.

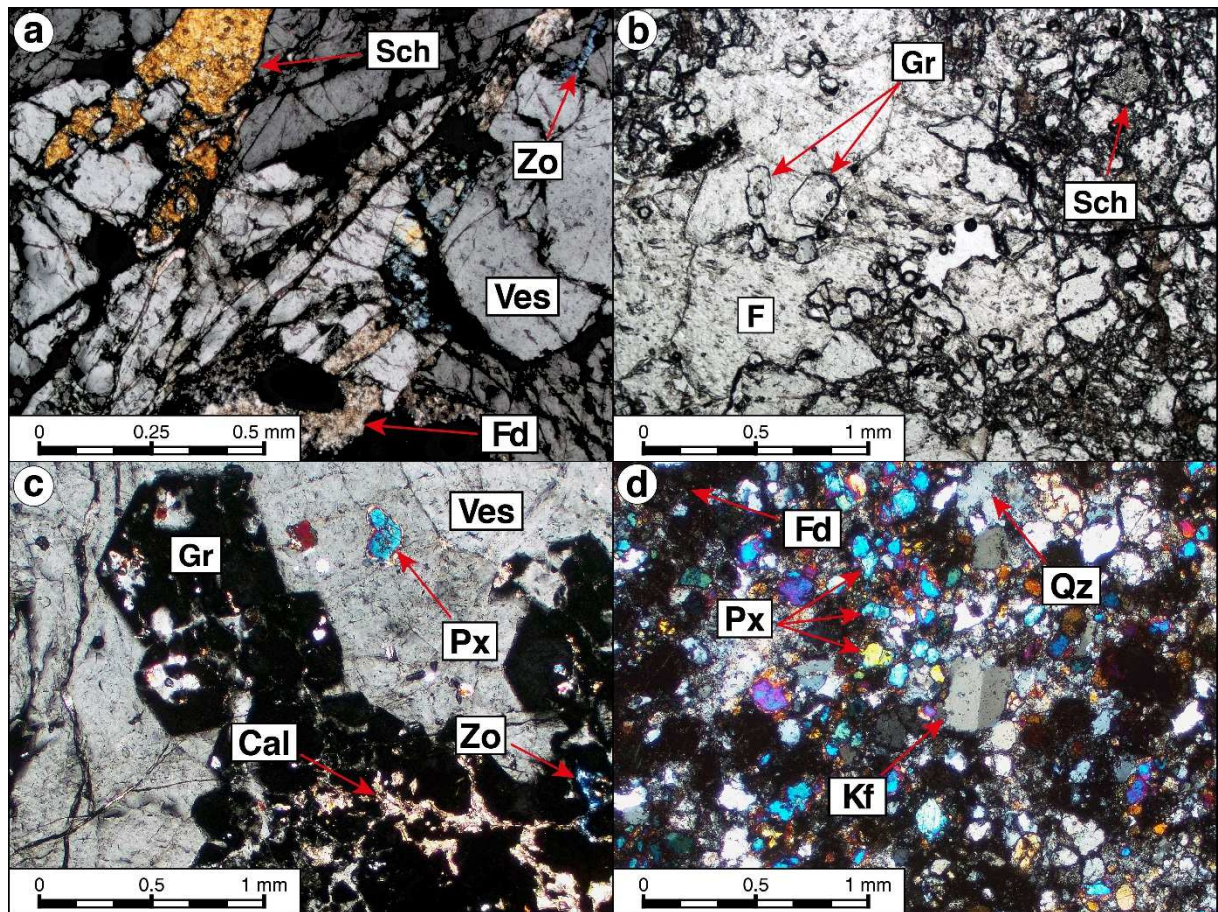


Fig. 2. Micrographs of thin sections of Main Skarn layer (a, b, c) and Lower Skarn layer (d) observed under **cross-polarised** light (a, c, d) and **polarised** light (b) with optical microscopy. Sch = Scheelite; F = Fluorite; Ves = Vesuvianite; Zo = Zoisite; Gr = Grossular; Px = Pyroxene; Cal = Calcite; Qz = Quartz; Fd = undetermined feldspars; Kf = K-feldspars.

3.2. Implications for the process

Due to the significant amount of S, often encountered in scheelite-skarn ores, **it is common** practice to perform a **sulphide** flotation stage prior to **scheelite** flotation (Tomas, 1985). In the Main Skarn, no sulphides were observed and, although some sulphides were identified in the Lower Skarn level, the choice was made to avoid any sulphide flotation in the present study. However, **particular** attention should be paid to the S grade in the Lower Skarn flotation concentrates.

The two **mineralised** layers both displayed relatively low liberations **sizes**, especially for the Lower Skarn. **The relatively high** density of scheelite (inducing high residence times in the ball mill) together

with its friability required care in fine grinding testwork to minimize the production of fine scheelite particles, resulting in unnecessarily high losses.

The Lower Skarn horizon was less challenging in terms of gangue mineral elimination given the dominance of easily depressed silicates such as quartz, feldspars or pyroxene and the lower abundance of fluorapatite, fluorite, and garnet. Hence, the following results focussed on the Main Skarn ore only.

Table 2. Comparison of the key mineralogical properties of the main minerals in the Main Skarn (magnetic susceptibility, specific gravity, and floatability with fatty acids) for the possible processing options for scheelite concentration. For each mineralogical property, the first sub-column gives the property value or class, while the second sub-column indicates the flow in which the mineral would be recovered. Dia.: diamagnetic, Conc.: concentrate, Para.: Paramagnetic, Tail.: Tailings, Mid.: Middlings.

Mineral	Class	Magnetic susceptibility		Specific gravity		Fatty-acids floatability	
		Class	Flow	Value	Flow	Value	Flow
Scheelite	Mineral of interest	Dia.	Conc.	6.1	Conc.	High	Conc.
Fluorite	Calcium salts	Dia.	Conc.	3.2	Mid.	High	Conc.
Apatite	Calcium salts	Dia.	Conc.	3.2	Mid.	High	Conc.
Vesuvianite	Dense silicates	Para.	Tail.	3.4	Mid.	Moderate	Mid.
Zoisite	Dense silicates	Para.	Tail.	3.4	Mid.	Moderate	Mid.
Grossular	Dense silicates	Para.	Tail.	3.7	Mid.	Moderate	Mid.
Quartz	Light silicates	Dia.	Conc.	2.7	Tail.	Low	Tail.
Feldspars	Light silicates	Dia.	Conc.	2.7	Tail.	Low	Tail.
Clay minerals	Light silicates	Para.	Tail.	2.6-3	Tail	Low	Tail.

Table 2 summarizes the Main Skarn’s mineralogical association, sorting the identified minerals in 4 different classes and displaying their respective properties (magnetic susceptibility, specific gravity, and floatability with fatty acids). Considering its mineralogical properties (Table 2), several beneficiation routes were investigated to produce a scheelite concentrate from the Main Skarn:

- (1) Gravity separation, which, based on the range of densities displayed by the various minerals, could provide efficient elimination of the light silicates (feldspars, quartz), reasonable rejection of calcium salts (fluorite, apatite), but poor rejection of the dense silicates (vesuvianite, zoisite, and grossular);

- (2) Magnetic separation that would lead to an efficient rejection of the paramagnetic minerals, namely, the dense silicates (vesuvianite, zoisite, and grossular);
- (3) Froth flotation with fatty acids, which would collect all the calcium minerals, namely, the calcium salts (scheelite, fluorite, and apatite) and the dense silicates (vesuvianite, zoisite, and grossular). However, the collection of the dense silicates and, to a lesser extent, of the unwanted calcium salts, can be addressed using specific depressants and new collector formulations.

The liberation size makes classical physical methods inefficient for scheelite beneficiation (Burt, 1999; Das and Sarkar, 2018), so the use of a Falcon centrifugal concentrator, specifically designed for fine particles gravity processing, was suggested for the Tabuaço skarn. Although the magnetic separation was also suitable for the Tabuaço skarn beneficiation, fine particles (+150-10 μm) cannot be processed in dry conditions, which is however appropriate for coarse particles only (>150 μm) and were then processed in wet conditions. Hence, magnetic separation was investigated on two different size fractions. Froth flotation was also tested on the fine particles (+150-10 μm), considering the fine liberation size. Since silicates represent 85-95 wt.% of the Tabuaço ore, the use of amines seemed inappropriate to attain good selectivity and the choice was made to work with fatty acids under the form of TOFA. However, the two mineralised layers of Tabuaço deposit, particularly the Main Skarn, displayed high amounts of calcium-bearing minerals, either calcium silicates or calcium semi-soluble salts (fluorite, apatite, calcite, and scheelite) which suggested the need for depressant optimisation and their dosage as well as the collector formulation.

3.3. Process optimisation for the Tabuaço skarn ore

Prior to the process optimisation, the milling stage was adapted to reach the liberation size avoiding scheelite losses in the fine particles. To attain this objective, the ball mill was fed with the retained fraction of a 150 μm sieve while the -150+0 μm fraction bypassed the milling stage. After milling, the product was sieved at 150 μm and the retained fraction constituted the circulating load (Fig. 3). The scheelite losses in the slimes (-10 μm) were assessed by analysing the WO_3 content of the hydrocyclone overflow when the feed was deslimed.

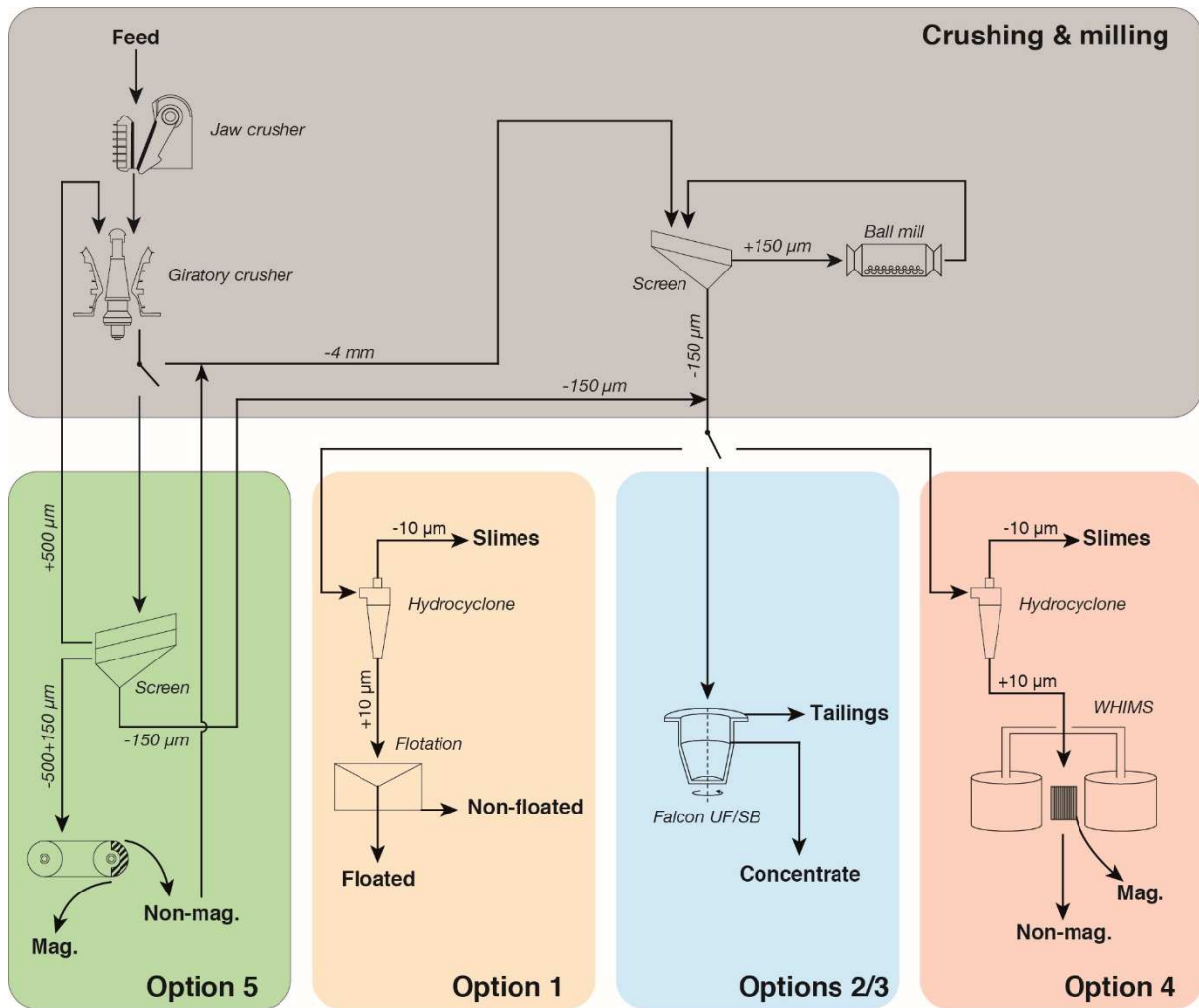


Fig. 3. Global flowsheet displaying the optimised milling stage and the 5 different options investigated for processing the Main Skarn Tabuaço ore. Options 1 to 4 are performed on a milled ore (-150 μm) while option 5 is performed prior to the milling stage. Options numbers correspond to the numbers introduced in the text.

Based on the mineralogical compositions (Table 1), the mineral properties (Table 2), and the previous discussions, 5 distinct beneficiation routes were suggested and investigated for the Main Skarn processing (Fig. 3):

- (1) Direct flotation,
- (2) Falcon UF gravity separation,
- (3) Falcon SB gravity separation,

(4) Wet high intensity magnetic separation,

(5) Dry high intensity magnetic separation performed on the unground -500+150 μm fraction.

Each route illustrated in Fig. 3 was optimised and all the processing options investigated were compared in terms of separation performances, with the global objective of combining the best routes to produce a marketable scheelite concentrate.

3.3.1. Depressants in direct flotation

The flotation with fatty acids used without depressant led to flotation of all the minerals, including scheelite, fluorite, apatite, and silicates (Filippov et al., 2018). Considering the very low separation efficiency between minerals, the use of depressants was mandatory in flotation. A previous study was conducted to find the best depressant(s) in terms of selectivity and WO_3 recovery (Foucaud et al., 2019b). Sodium silicate, commonly used for gangue mineral depression, especially for silicates, exhibited poor fluorite depression. Several depressants were then tested to improve the flotation selectivity (Fig. 4). The effect of adding metallic salts (iron, zinc, and aluminium salts) prior to sodium silicate was studied as well as the sole use of organic molecules (citric acid, carboxymethyl cellulose, tannin, lignin sulfonate, and starch). Among all the depressants investigated, the combination of sodium carbonate and sodium silicate exhibited the best efficiency (Fig. 4), mainly attributed to strong positive synergistic effects existing between the two reagents (Agar, 1984; Foucaud et al., 2019b).

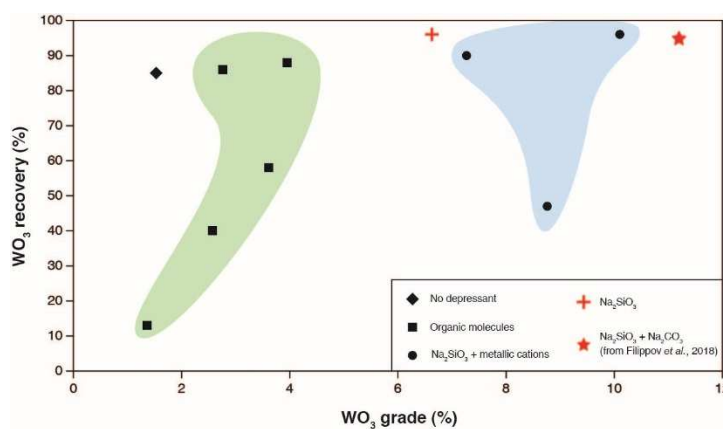


Fig. 4. WO_3 recovery as a function of WO_3 grade for the different tested depressants, from (Foucaud et al., 2019b).

Both the WO_3 grade and recovery were optimised through a 4-level factorial design of experiments, commonly used for optimisation work. However, the approach using depressants was limited: fluorite and scheelite display very close distances between the surface calcium atoms inducing a very low selectivity of all the depressants, particularly when they occur in large molecules with high surface coverage.

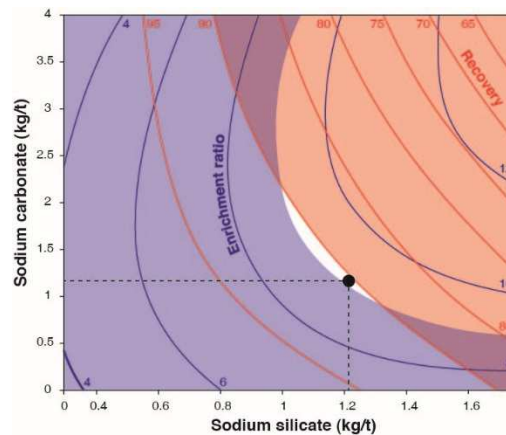


Fig. 5. Iso-response surface of the WO_3 enrichment ratio and WO_3 recovery as a function of sodium silicate and sodium carbonate, from (Foucaud et al., 2019b). The area in white is the optimal field where the best quantities are defined: ~ 1.225 kg/t sodium silicate and 1.150 kg/t sodium carbonate.

The optimised conditions for maximising both WO_3 grade and recovery were 1.150 kg/t sodium carbonate and 1.225 kg/t sodium silicate with 200 g/t of RBD15 as collector, according to the iso-response graph drawn following the WO_3 enrichment ratio and recovery modelled by the design of experiments (Fig. 5). The test with optimised depressing conditions was performed again in the present study, see Table 3. First, slimes represented 6.3% WO_3 loss, which was an acceptable value indicating that no scheelite concentration occurred in the fine particles during grinding. The concentrate product of a one-stage flotation on this deslimed ore assayed 9.2% WO_3 with 87.8% WO_3 recovery for a feed assaying 1.1% WO_3 , which was in agreement with the validation test performed in (Foucaud et al., 2019b). Both dense and light silicates as well as apatite were efficiently depressed since the Fe_2O_3 , K_2O , and P_2O_5 recoveries in the concentrate were 3.8%, 2.4%, and 26.9%, respectively (Table 3). Very few silicates and apatite particles could be observed in the flotation concentrate product (Fig. 6). However, the fluorite recovery in the concentrate product remained unacceptably high at 55.1% (Table 3),

illustrating that, even with high sodium carbonate/sodium silicate concentrations, fluorite could not be efficiently depressed and represented most of the concentrate product (Fig. 6), diluting dramatically the WO_3 content. Particles were mostly free and no mineral association was observed between scheelite and fluorite: the flotation selectivity depended then only on the selectivity of the reagents. The following discussions will use the “optimised depressants” designation for the test performed with 1.150 kg/t sodium carbonate and 1.225 kg/t sodium silicate.

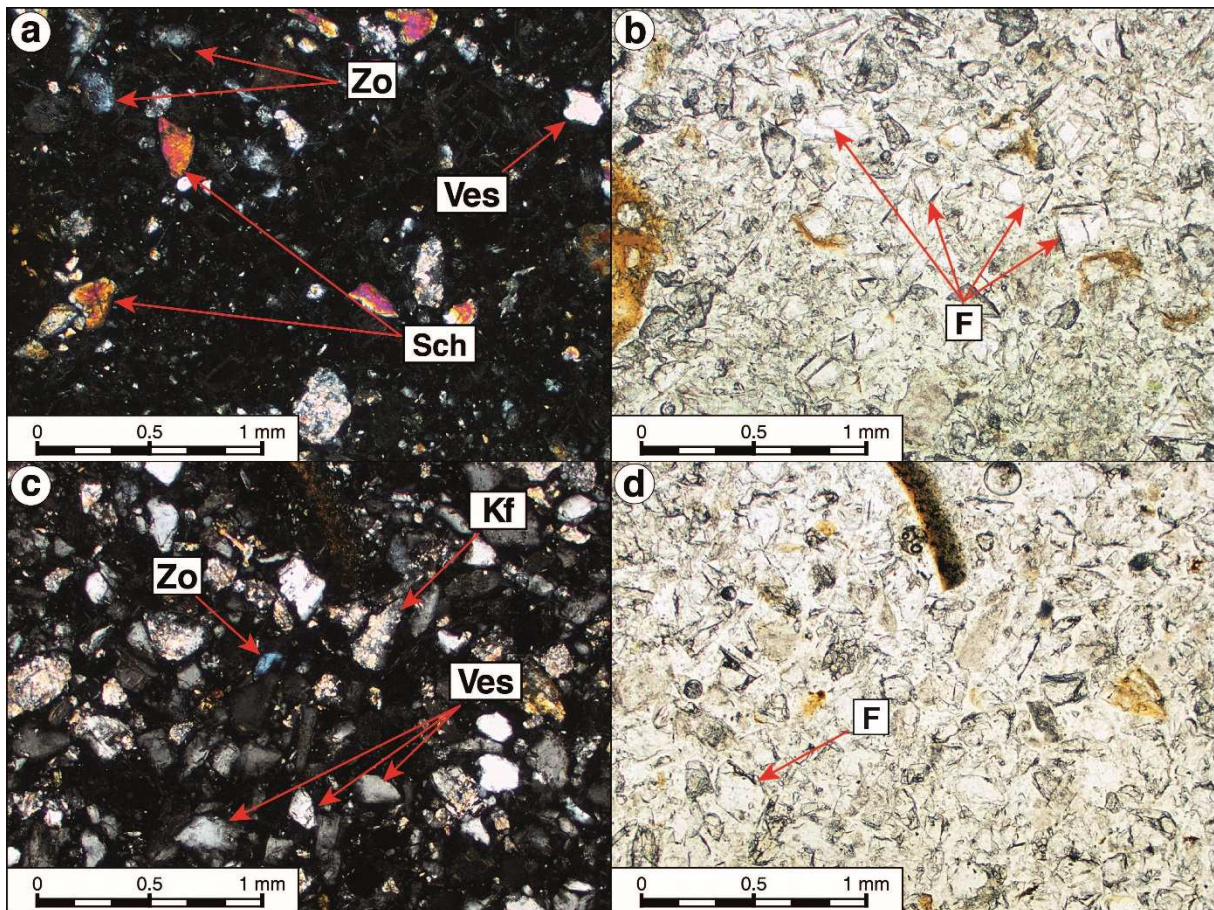


Fig. 6. Micrographs of thin sections of the concentrate (a, b) and the tailings (c, d) of the flotation test with optimised depressants conditions observed with an optical microscope under cross-polarised light (a, c) and polarised light (b, d). Abbreviations defined in Fig. 2 caption.

3.3.2. Flotation collectors

Previous results suggested that the depressants currently available did **not enhance** significantly the selectivity between scheelite and fluorite. Hence, under the best depressing conditions, the main focus was put on the collectors: a good separation contrast could not be attained with RBD15, mainly composed of oleic and linoleic acids which are mono- and bi-unsaturated fatty acids, respectively. They are widely used for their vegetal origin and their low fusion temperatures, making them easy to use at room temperature. We reported in a previous study that the introduction of saturated fatty acids in the oleic-linoleic-acids-based formulations **significantly enhanced the** selectivity between scheelite and fluorite in flotation (Filippov et al., 2018). It was assumed that the saturated fatty acids led to a better organisation of the adsorption layer. They decreased the dependence of the organisation on the collectors' geometries and **maximised** the influence of the crystallographic properties, **thus exploiting fine** differences existing between the two minerals. Consequently, LD, a new TOFA containing a significant part of saturated fatty acids, was used in the present study. With the optimised depressants conditions, the collector formulation and quantity were optimised in the aforementioned previous study, **allowing optimal** conditions at 600 g/t of LD (Filippov et al., 2018). This test was performed again in the present study and produced a flotation concentrate assaying 14.1% WO₃ with 77.1% WO₃ recovery for a feed assaying 1.1% WO₃ (Table 3). Compared to the test with RBD15, the WO₃ recovery in the concentrate was significantly reduced, from 87.9% to 77.1% while the F recovery was decreased from 55.1% to 32.9%, as well as the other gangue minerals recoveries, see Table 3. **LD produced a WO₃ grade that** was 1.5 times **higher than when RBD15** was used (14.1% WO₃ instead of 9.2% WO₃). The following discussions will use the “fully-optimised flotation” or “optimised depressants and collectors” designations for the test performed with 1.150 kg/t sodium carbonate, 1.225 kg/t sodium silicate and 600 g/t LD.

Table 3. Material balances of the two flotation schemes, using either RBD15 or LD as collectors with optimised depressants. Product names correspond to those defined in Fig. 3.

Product	wt.%	WO ₃ grade (%)	WO ₃ recovery (%)	P ₂ O ₅ recovery (%)	K ₂ O recovery (%)	Fe ₂ O ₃ recovery (%)	F recovery (%)
<i>RBD15</i>							
Slimes	7.5	0.9	6.3	5.0	14.9	11.3	7.3
Non-floated	82.5	0.1	5.8	68.1	82.7	84.9	37.6
Floated	10.0	9.2	87.9	26.9	2.4	3.8	55.1
Feed*	100.0	1.1	100.0	100.0	100.0	100.0	100.0
<i>LD</i>							
Slimes	7.5	0.9	6.9	5.3	13.4	12.0	7.7
Non-floated	87.3	0.2	16.0	89.1	85.8	85.5	59.4
Floated	5.2	14.1	77.1	5.6	0.8	2.4	32.9
Feed*	100.0	1.1	100.0	100.0	100.0	100.0	100.0

* Feed is back-calculated

3.3.3. Falcon gravity separation

Another beneficiation route investigated for the Tabuaço ore was to take advantage of the significant specific gravity contrast existing between scheelite (6.1) and fluorite (3.2), the latter being the most problematic mineral in flotation with a recovery as high as 35.7% in the fully-optimised-flotation step. Hence, the use of a Falcon concentrator to eliminate the fluorite by gravity separation prior to or after flotation was investigated. Two types of Falcon bowls, Falcon UF and Falcon SB, were employed and compared. The Falcon UF is specifically designed to recover ultrafine particles, while the Falcon SB allows a fluidisation counter-pressure to be injected in the trapping gutters to wash the concentrate. A previous study optimised the operating parameters for the two bowls following the design of experiments method (Foucaud et al., 2019a). Tests with these optimised operating parameters were performed in the present study with Falcon UF and Falcon SB, see Table 4.

Table 4. Material balances of the Falcon UF and Falcon SB optimised experiments. Product names correspond to those defined in Fig. 3.

Product	wt.%	WO ₃ grade (%)	WO ₃ recovery (%)	P ₂ O ₅ recovery (%)	K ₂ O recovery (%)	Fe ₂ O ₃ recovery (%)	F recovery (%)
<i>Falcon UF</i>							

Tailings	78.6	0.6	44.0	74.1	81.9	78.3	78.7
Concentrate	21.4	2.8	56.0	25.9	18.1	21.7	21.3
Feed*	100.0	1.1	100.0	100.0	100.0	100.0	100.0
<i>Falcon SB</i>							
Tailings	84.2	0.3	24.2	79.7	88.5	84.3	84.7
Concentrate	15.8	5.0	75.8	20.3	11.5	15.7	15.3
Feed*	100.0	1.1	100.0	100.0	100.0	100.0	100.0

* Feed is back-calculated

The Falcon SB rejected 84.7% and 79.7% of the total amounts of fluorite and apatite, respectively, from the concentrate with 75.8% WO₃ recovery in the concentrate (Table 4). Although the silicates (both dense and light) were efficiently rejected, vesuvianite still represented, with scheelite, most of the Falcon SB concentrate (Fig. 7). Consistently, the tailings mostly comprised fluorite, light silicates, and fine particles (Fig. 7). The Falcon SB concentrate yielded 15.8 wt.% of the total feed, which means that it rejected 84.2 wt.% of the total feed (Table 4). The Falcon UF exhibited lower performances in terms of WO₃ recoveries, gangue minerals' rejection, and, consequently, WO₃ grade (Table 4). Besides, Falcon bowls allowed an efficient desliming of the pulp as Falcon UF displayed **slime rejection performance similar to a hydrocyclone** (around 50% of desliming efficiency) while the Falcon SB eliminated 95% of the slimes (Foucaud et al., 2019a), see Fig. 7.

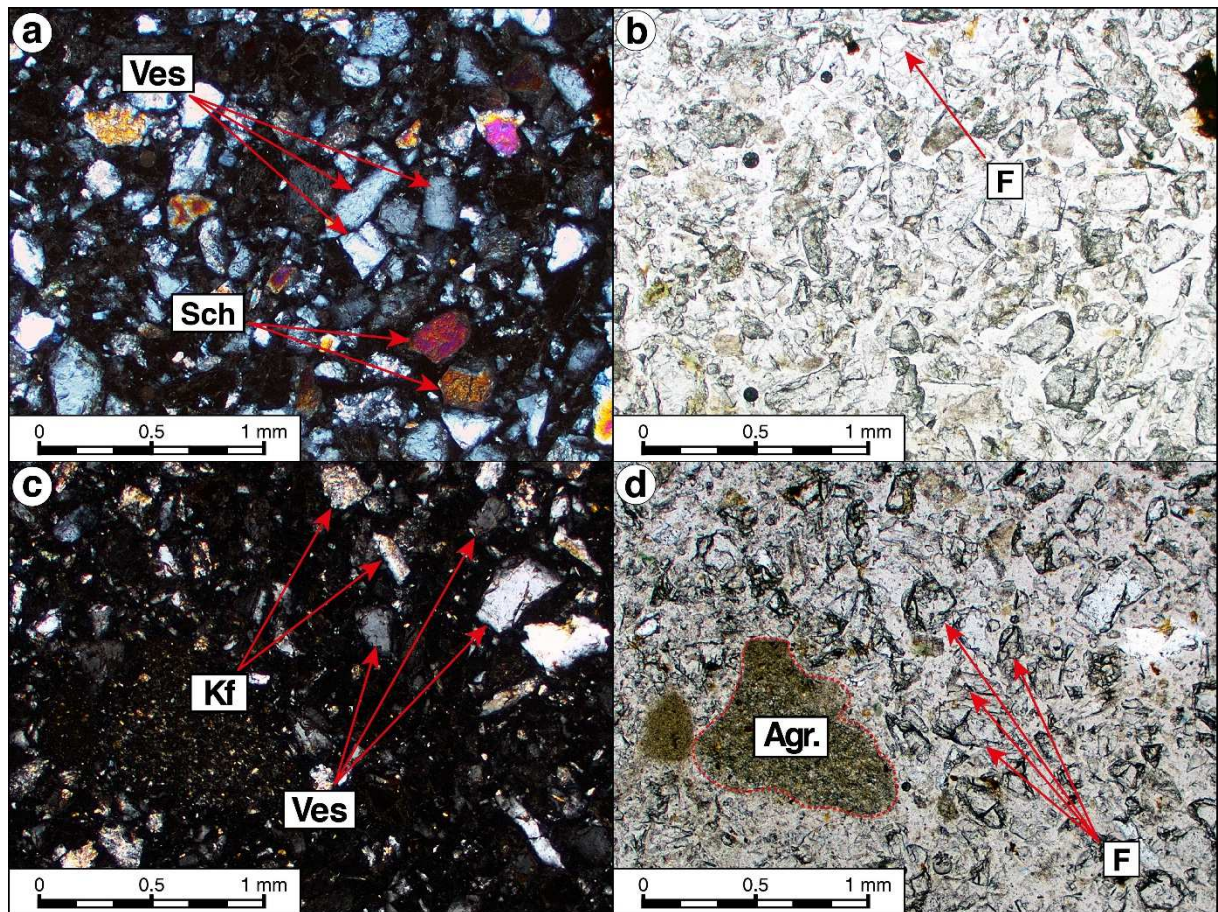


Fig. 7. Micrographs of thin sections of the concentrate (a, b) and the tailings (c, d) of the Falcon SB test with optimised operating parameters observed with optical microscope under **cross-polarised** light (a, c) and **polarised** light (b, d). Abbreviations defined in Fig. 2 and 3 captions, Agr = Aggregate, *i.e.* aggregates fine particles.

3.3.4. High intensity magnetic separation

The Tabuaço W-skarn contained high amounts of vesuvianite, which comprises iron and magnesium (Table 1), and significant amounts of zoisite and grossular that also include iron and magnesium (Table 1). Overall, more than 70 wt.% of the Main Skarn and 90 wt.% of the Lower Skarn were ferromagnesian minerals that are paramagnetic. These minerals corresponded to the dense silicates that were not eliminated by the Falcon separation but very efficiently by froth flotation, see section 3.3.1. Hence, magnetic separation was a possible option to eliminate the dense silicates in addition to the flotation stage. Both dry and wet high intensity magnetic separations were tested on the Main Skarn. However, the dry magnetic separation is known to be inefficient on fine particles and was then performed on

the -500+150 μm fraction, prior to the milling stage, while the wet magnetic separation was performed on the flotation feed, namely, the -150+10 μm fraction.

The results of the magnetic separation tests are presented in Table 5. The magnetic and non-magnetic products of the dry magnetic separation were observed under optical microscope to estimate the behaviour of each mineral (Fig. 8). The dry magnetic separation exhibited satisfying results (Table 5): the magnetic fraction comprised mainly the ferromagnesian minerals, corresponding to the dense silicates, namely, vesuvianite, zoisite, and grossular (Fig. 8). The non-magnetic fraction was composed of calcium salts (scheelite, fluorite, and apatite) and non-ferromagnesian silicates such as quartz and feldspars (Fig. 8). As illustrated in Fig. 3, the 0-150 μm fraction, separated prior to the dry magnetic separation, constituted a part of the flotation/Falcon feed and was then not considered as tailings. Hence, only the magnetic fraction corresponded to a tailing product. It represented 44.5 wt.% of the total yield with 6.0% WO_3 recovery, 13.7% P_2O_5 recovery, 25.8% K_2O recovery, 59.6% Fe_2O_3 recovery, and 27.8% F recovery demonstrating an efficient rejection of the dense ferromagnesian silicates (Table 5). The P_2O_5 , K_2O , and F recoveries in the magnetic fraction were significantly higher than the WO_3 recovery, suggesting that apatite, fluorite, and light silicates, which did not display paramagnetic properties, were more likely to be associated with ferromagnesian minerals than scheelite. Overall, this test demonstrated that a dry, high intensity magnetic separation stage would reduce the mass fed to the milling stage by 44.5 wt.%, with limited scheelite losses, namely 6.0%. Moreover, most of the rejected minerals, *i.e.*, the dense ferromagnesian silicates, exhibit high hardness that would negatively impact the milling stage.

Table 5. Material balances of the dry and wet magnetic separation tests, which are performed on different feed products, as reported in Fig. 3. Product names correspond to those defined in Fig. 3.

Product	wt.%	WO_3 grade (%)	WO_3 recovery (%)	P_2O_5 recovery (%)	K_2O recovery (%)	Fe_2O_3 recovery (%)	F recovery (%)
<i>DHIMS</i>							
0-150 μm	35.6	1.0	33.6	43.4	26.2	33.6	22.7
Mag.	44.5	0.2	6.0	13.7	25.8	59.6	27.8
Non-mag.	19.9	3.3	60.4	42.9	48.0	6.8	49.5

Feed*	100.0	1.1	100.0	100.0	100.0	100.0	100.0
<i>WHIMS</i>							
Slimes	7.5	0.9	7.9	6.5	14.0	11.4	7.7
Mag.	33.4	0.2	7.2	10.4	10.7	45.5	15.6
Non-mag.	59.2	1.2	84.9	83.1	75.3	43.1	76.7
Feed*	100.0	0.9	100.0	100.0	100.0	100.0	100.0

* Feed is back-calculated

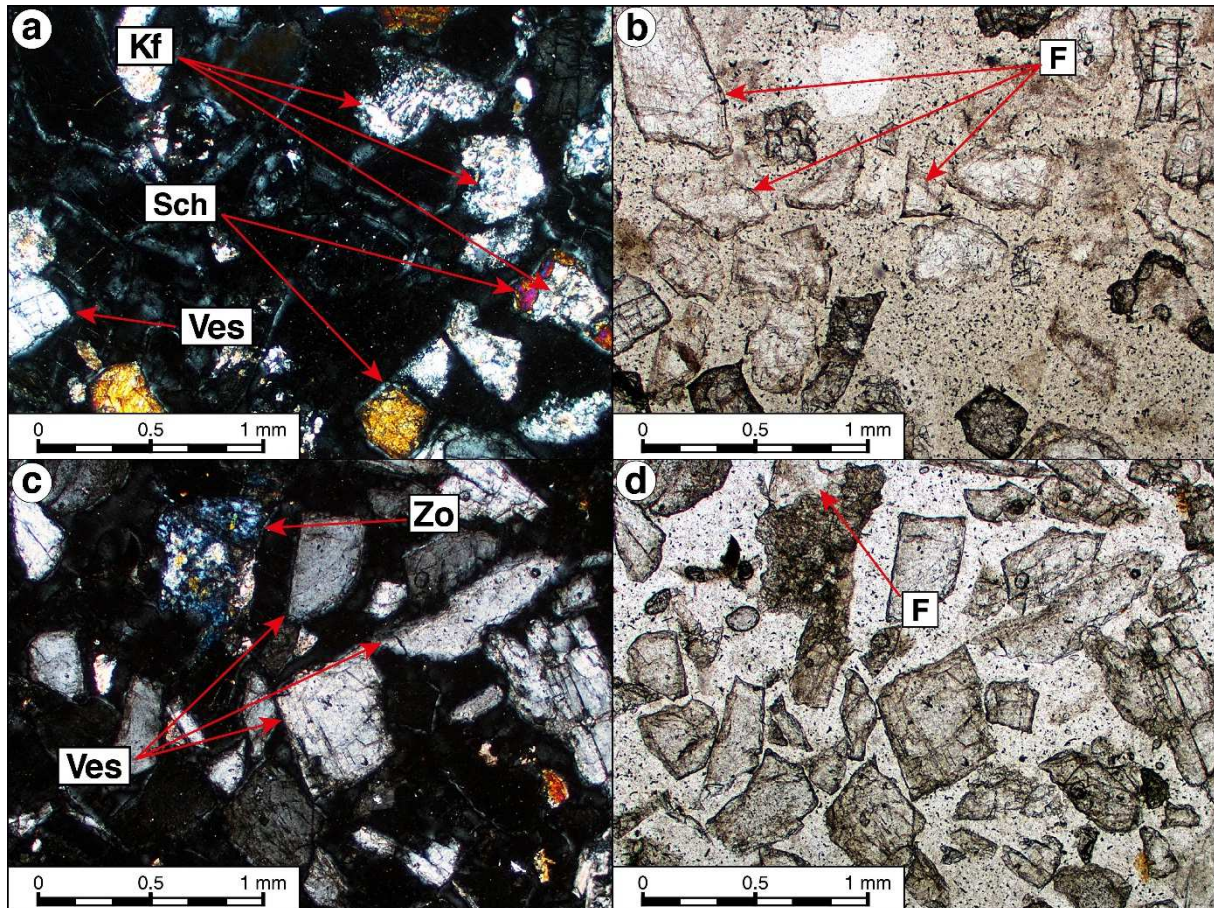


Fig. 8. Micrographs of thin sections of the concentrate, i.e. the non-magnetic product, (a, b) and the tailings, i.e. the magnetic product, (c, d) of dry high intensity magnetic separation with optimised operating parameters observed with optical microscope under **cross-polarised** light (a, c) and **polarised** light (b, d). Abbreviations defined in Fig. 2 and 3 captions.

The wet magnetic separation displayed significantly lower performances compared to the dry magnetic separation, despite the different processed fractions (Table 5). Hereby, the slimes and the magnetic product were considered as tailings, as illustrated in Fig. 3. The non-magnetic product represented 59.2 wt.% of the mass, with 84.9% WO_3 recovery, 83.1% P_2O_5 recovery, 75.3% K_2O recovery,

43.1% Fe₂O₃ recovery, and 76.7% F recovery (Table 5). The WO₃ recovery was lower compared to the dry magnetic separation, mainly due to losses in slimes, while the gangue minerals rejection compared poorly with the dry magnetic treatment option.

3.3.5. Combination of gravity and flotation

The Falcon UF exhibited performances significantly lower than the Falcon SB (see section 3.3.3.), which, additionally, displayed a very satisfying rejection of fluorite that was problematic in flotation with fatty acids. Consequently, the Falcon SB was selected to be combined with flotation, as a pre-concentrating or a post-concentrating apparatus. Besides, flotation cleaning stages were performed to enhance the WO₃ grade of the concentrate. Since the use of LD provided an increase in the WO₃ grade but a decrease in the WO₃ recovery, the choice was made to test the two types of flotations, either with RBD15 or with LD, at optimised depressing conditions for both. Finally, considering the performances of magnetic separation, this latter option was not able to supplant flotation and the choice was made not to combine it with other separation techniques although it would provide rejection of 44.5 wt.% of the yield prior to the milling stage.

Based on the results of each separation performed separately and the previous discussions, several global flowsheets were suggested and tested (Fig. 9):

- (1) 2-steps flotation with optimised depressants,
- (2) 2-steps flotation with optimised depressants and collectors (*i.e.* LD),
- (3) Falcon SB concentration followed by flotation with optimised depressants,
- (4) Falcon SB concentration followed by flotation with optimised depressants and collectors (*i.e.* LD),
- (5) Flotation with optimised depressants followed by Falcon SB concentration.

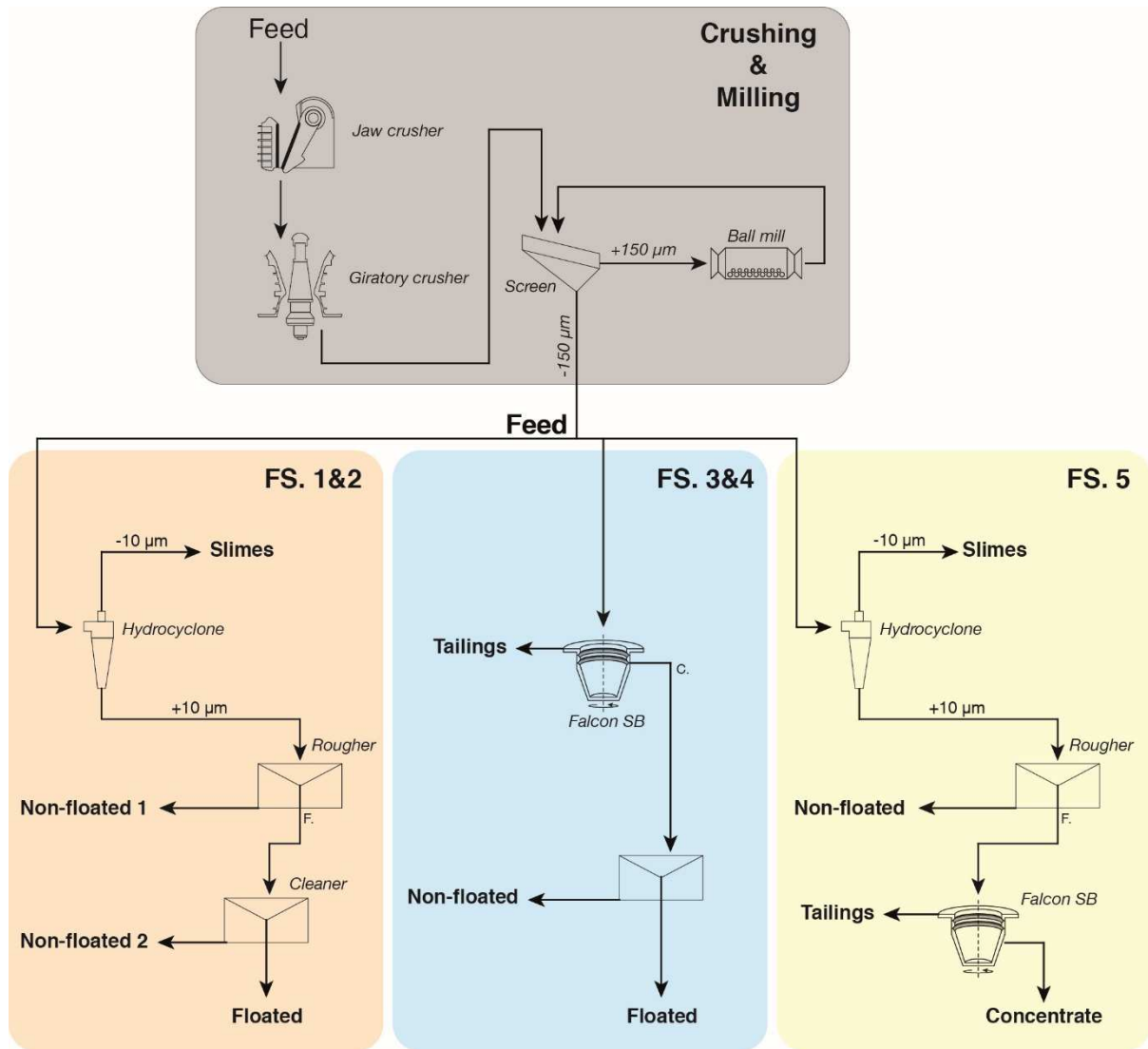


Fig. 9. Overview of the 5 distinct flowsheet (FS) investigated in this study for the Tabuaço skarn ore.

Results in terms of WO_3 grade and recovery for each flowsheet are presented in Fig. 10 while the detailed material balances are presented in Table 6. The flowsheets incorporating only froth flotation exhibited significantly higher WO_3 grade when LD was used, with similar WO_3 recovery (FS. 1&2). The Falcon SB pre-concentrate displayed a significantly lower WO_3 grade and recovery than the flotation concentrate (Table 6). However, most of the fluorite and the apatite were eliminated from the pre-concentrate, as well as most of the slimes. It induced a very high efficiency, *i.e.* enrichment ratio, of the subsequent flotation stage, performed on the Falcon SB pre-concentrate. The final concentrate, after only two separation stages (Falcon SB followed by flotation with RBD15) assayed 38.1% WO_3 with 62.5% WO_3 global recovery (Fig. 10) from a feed assaying 1.1% WO_3 (Table 6). Moreover, the yield after the Falcon SB stage was 15.1-15.8 wt.%, meaning that around 85 wt.% of the total feed mass was

rejected during this phase. When the flotation with LD was performed on the Falcon SB pre-concentrate, the results were roughly the same (Table 6), attributed to the fact that most of the fluorite was rejected by the Falcon separation. This prior rejection erased the selectivity differences between RBD15 and LD, producing then very similar concentrates. However, the use of LD increased slightly the WO_3 recovery, probably due to higher dosages compared to RBD15 (600 g/t instead of 200 g/t).

The reverse flowsheet has also been tested where the final concentrate, after a flotation stage with RBD15 followed by a Falcon SB stage, assayed 25.9% WO_3 with 55.9% WO_3 global recovery (Fig. 10, Table 6). This option however presented fewer advantages: (1) when the flotation was performed first, the ore had to be deslimed and then required the use of a hydrocyclone, implying more operations and scheelite losses in the slimes; (2) since the Falcon represents lower operating costs compared to flotation, the highest flowrates should be processed with the Falcon and (3) the fatty acids did not desorb from the particles surfaces and made the scheelite and fluorite particles hydrophobic, which disturbed the separation mechanisms during the Falcon stage performed on the flotation concentrate.

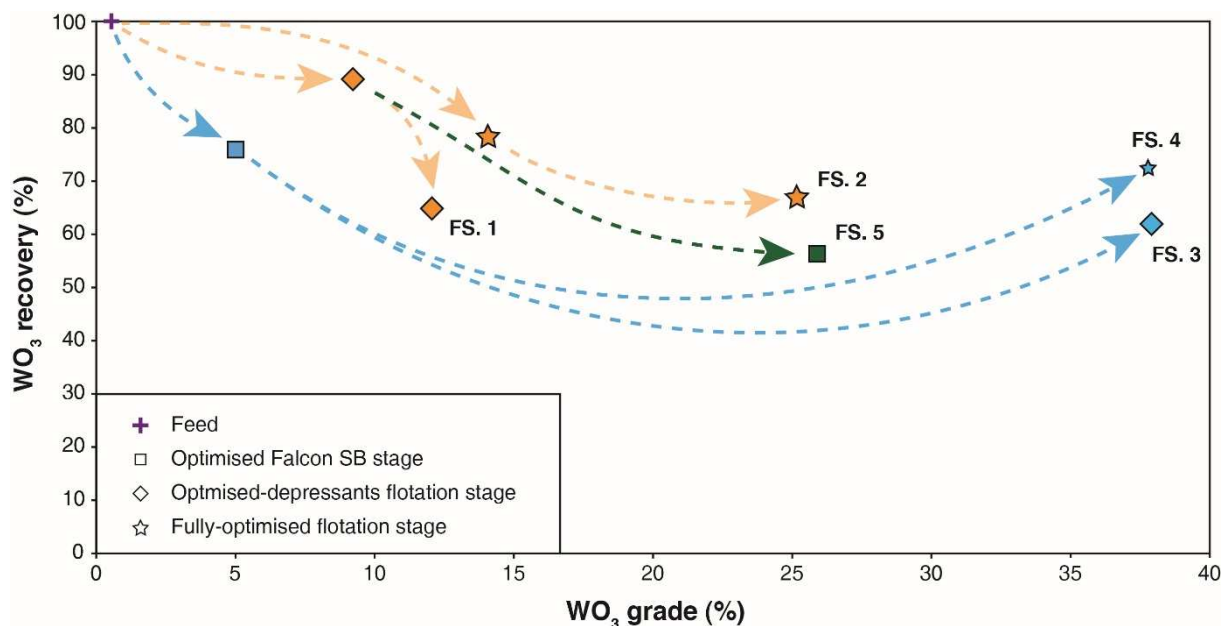


Fig. 10. WO_3 recovery - WO_3 grade curve displaying the different flowsheets investigated for the beneficiation of the Main Skarn layer at Tabuaço deposit. The hydrocyclone stage is included in the flotation stage when this latter process is performed first, the WO_3 recoveries take into account the losses in the slimes. Flowsheets numbers and colours correspond to those of Fig. 9.

Table 6. Material balances of the 5 different flowsheets investigated for the beneficiation of the Main Skarn layer. Flowsheets numbers and product names correspond to those defined in Fig. 9.

Product	wt.%	WO ₃ grade (%)	WO ₃ recovery (%)	P ₂ O ₅ recovery (%)	K ₂ O recovery (%)	Fe ₂ O ₃ recovery (%)	F recovery (%)
<i>Flotation (RBD15)</i>							
Slimes	7.5	0.9	6.3	5.0	14.9	11.3	7.3
Non-floated 1	82.5	0.1	5.8	68.1	82.7	84.9	37.6
Non-floated 2	4.4	5.7	23.7	18.1	2.1	2.9	14.7
Floated	5.6	12.0	64.2	8.8	0.3	0.9	40.5
Feed*	100.0	1.1	100.0	100.0	100.0	100.0	100.0
<i>Flotation (LD)</i>							
Slimes	7.5	0.9	6.9	5.3	13.4	12.0	7.7
Non-floated 1	87.26	0.2	16.0	89.1	85.8	85.5	59.4
Non-floated 2	2.7	3.9	11.2	1.9	0.8	1.8	16.7
Floated	2.5	25.2	66.0	3.7	0.0	0.6	16.2
Feed*	100.0	1.0	100.0	100.0	100.0	100.0	100.0
<i>Falcon SB → Flotation (RBD15)</i>							
Falcon tailings	84.2	0.3	24.2	79.7	88.5	84.3	84.7
Non-floated	14.1	1.0	13.3	15.4	11.5	15.2	8.6
Floated	1.7	38.1	62.5	4.9	0.0	0.5	6.7
Feed*	100.0	1.1	100.0	100.0	100.0	100.0	100.0
<i>Falcon SB → Flotation (LD)</i>							
Falcon tailings	84.9	0.3	23.7	79.0	89.4	85.2	85.0
Non-floated	13.1	0.3	3.7	13.0	10.4	14.2	8.0
Floated	2.0	37.8	72.6	8.0	0.2	0.6	7.0
Feed*	100.0	1.0	100.0	100.0	100.0	100.0	100.0
<i>Flotation (RBD15) → Falcon SB</i>							
Slimes	7.5	0.9	6.1	6.2	13.2	11.9	7.8
Non-floated	81.6	0.1	10.2	66.7	83.4	82.4	37.3
Falcon tailings	8.6	3.5	27.8	18.8	3.1	4.8	44.7
Falcon conc.	2.3	25.9	55.9	8.3	0.3	0.8	10.2
Feed*	100.0	1.1	100.0	100.0	100.0	100.0	100.0

* Feed is back-calculated

Based on the WO₃ grade and recovery, the flowsheet 4 (Falcon SB → Flotation with LD) was selected as the best option for the Tabuaço Main Skarn processing since it produced a final concentrate assaying 37.8% WO₃ with an overall 72.6% WO₃ recovery. Several cleaning stages were performed on the concentrate of this test, without additional reagent addition (Fig. 11). Undoubtedly, successive cleaning stages increased the WO₃ grade with a moderate decrease of the WO₃ recovery. After 4 flotation stages performed on the Falcon SB pre-concentrate, the final concentrate assayed 62.9% WO₃ for 59.4% WO₃

recovery from the feed assaying 1.1% WO_3 (Fig. 11), which constituted a marketable scheelite concentrate.

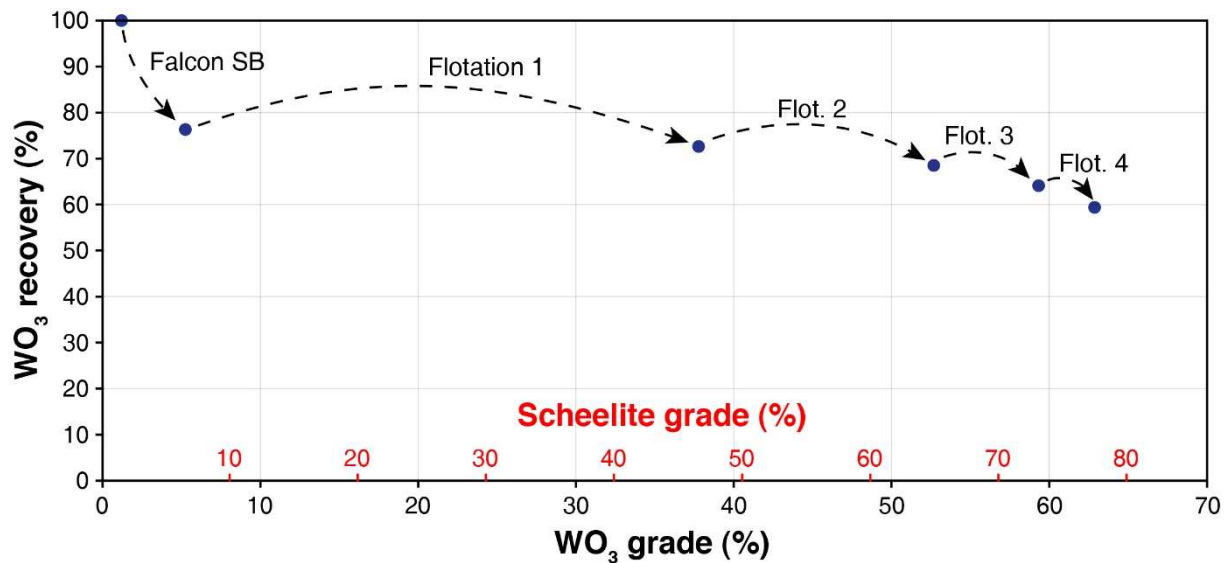


Fig. 11. WO_3 recovery vs. WO_3 and scheelite grades for the best flowsheet showing the influence of the Falcon SB and the flotation stages on the WO_3 grade and recovery.

4. Economic assessment and conclusions

The present study aimed to recover tungsten from a typical complex skarn ore, adapting the process to the mineralogy of the ore. The integrated flow-sheet developed here is presented on Fig. 12. First, we demonstrated that a dry magnetic separation was a possible option on the crushed feed prior to fine grinding. It would lead to the rejection, prior to the milling stage, of around 45 wt.% of the yield that mainly contain the hardest minerals of the ore (dense ferromagnesian silicates), which would correspond to a significant energy saving. The magnetic fraction contained only 6.0% of the total scheelite distribution and could be considered as tailings.

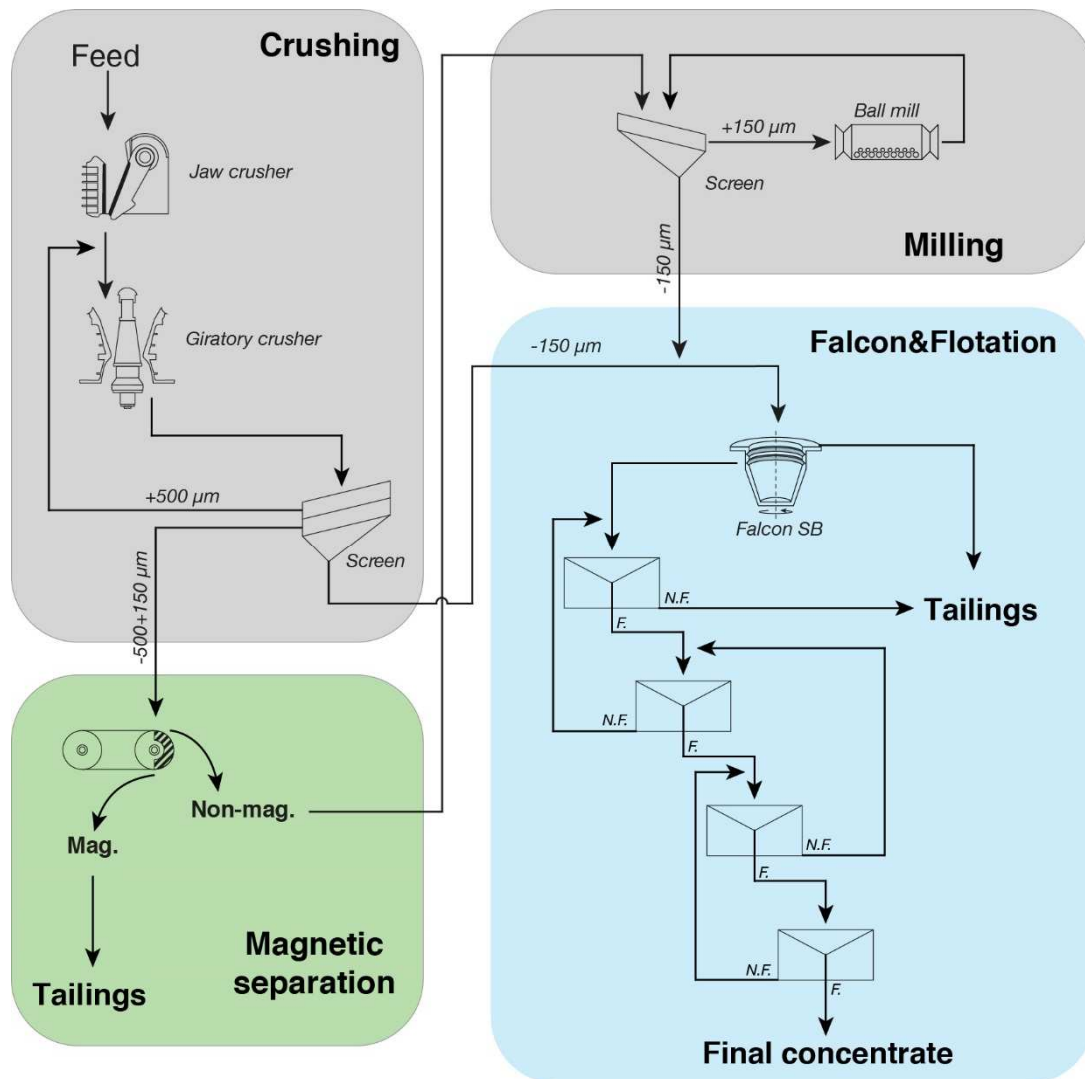


Fig. 12. Suggested global flow-sheet for the production of a marketable scheelite concentrate for the Main Skarn level.

Moreover, the use of a Falcon SB prior to flotation provided: (1) rejection of around 85 wt.% of the total milled feed, (2) desliming with a high efficiency for the flotation feed and, (3) after only one fully-optimised flotation stage, producing a concentrate assaying 37.8% WO_3 with 72.6% WO_3 global recovery. This process route was better than a two-stage flotation that produced a concentrate assaying 12.0% with 64.2% WO_3 recovery with RBD15 or assaying 25.2% WO_3 with 66.0% WO_3 recovery for novel reagents formulations (LD), see Fig. 10 and Table 6. Performing several flotation stages on the Falcon SB pre-concentrate produced a concentrate assaying 62.9% WO_3 with 59.4% WO_3 global recovery, which was a marketable scheelite concentrate. The WO_3 recovery would be significantly increased if the integrated process was scaled-up from batch tests, performed in the present study, to

continuous scale (*i.e.* pilot scale) since **the tailings** products, containing significant amounts of scheelite, would be recirculated (Fig. 12). Moreover, studies on the Falcon SB tailings, which still represented around 24% WO₃ distribution, could be **undertaken** to increase **the overall WO₃ recovery**.

The flowsheets developed **here** could be adapted to the targeted performance: the operating parameters used for the Falcon SB stage could be defined to **maximise** either the gangue minerals (mostly fluorite) rejection, *i.e.* the WO₃ grade or the WO₃ recovery (Foucaud et al., 2019a). Furthermore, the number of flotation cleaning stages performed on the Falcon SB pre-concentrate could be **optimised** to **maximise** the WO₃ grade or the WO₃ recovery.

Overall, the suggested flowsheets **would**:

- Reduce the energy consumption as more than half of the product is rejected before the mill,
- Reduce the reagents costs, decreasing the ore quantity processed by flotation,
- Reduce the energy/water consumption as less feed material is sent to flotation,
- Use only **environmental benign** chemicals in flotation (Na₂CO₃, Na₂SiO₃, fatty acids) as problematic gangue minerals are eliminated before flotation,
- Produce a marketable WO₃ concentrate (62.9% WO₃),
- Adapt the processing route to the product specifications or to the targeted performance (WO₃ grade or WO₃ recovery).

Approximatively 375 000 tons/year would be processed in the Tabuaço plant, which represents 45 t/h. The adapted Falcon concentrator has a motor power of 30 kW which represents, given the average electricity price of 0.21 €/kWh in Portugal, 6.3 €/h and thus 0.14 €/t. No water is required after the milling stage as the Falcon can process pulps at more than 30% wt. solids. It represents extremely low operating costs compared to the flotation stage. Even if the flotation cells energy consumption is similar to the Falcon one, flotation needs the addition of water to reach 30 % wt. solids in the pulp and requires reagents that constitute an important part of the operating costs. Globally, the implementation of a Falcon concentrator in the process leads to the elimination of around 85 wt.% of the total feed flowrate, **resulting in a flotation feed stream of** only 7.2 t/h instead of 45 t/h. Assuming 250 €/ton for the Na₂CO₃,

150 €/ton for the Na₂SiO₃ and 700 €/ton for the TOFA, the gravity pre-concentration leads to a saving of approximately 20 €/h and then 0.45 €/t. Further, the implementation of a dry magnetic separation prior to the milling stage would lead to the rejection of around 45 wt.% of the total feed flowrate, inducing that the energy consumed for the milling would be 2 times lower. Overall, the process choice should be adapted to the ore characteristics as new methods exist for on-line monitoring and for selective mining following integrated approaches.

Acknowledgements

The research leading to these results has received funding from the FAME project under European Union's Horizon 2020 research and innovation program [grant agreement No 641650]. We also acknowledge the support of Labex Ressources 21, supported by the French National Research Agency through the national program “Investissements d’Avenir” [reference ANR-10-LABX-21]. We would finally like to thank the STEVAL platform and its technical staff who was closely involved in this work.

References

- Abeidu, A.M., 1973. Selective depression of calcite from fluorite. Transactions of the Institution of Mining and Metallurgy, Section C 49–50.
- Agar, G.E., 1984. Scheelite Flotation Process. US Patent 4,488,959.
- Arnold, R., Brownbill, E.E., Ihle, S.W., 1978. Hallimond tube flotation of scheelite and calcite with amines. International Journal of Mineral Processing 5, 143–152. [https://doi.org/10.1016/0301-7516\(78\)90011-X](https://doi.org/10.1016/0301-7516(78)90011-X)
- Atademir, M.R., Kitchener, J.A., Shergold, H.L., 1979. The surface chemistry and flotation of scheelite. I. Solubility and surface characteristics of precipitated calcium tungstate. Journal of Colloid and Interface Science 71, 466–476.
- Audion, A.S., Labbé, J.F., 2012. Panorama 2011 du marché du tungstène.
- Blazy, P., Joussemet, R., 2011. Concentration par gravité - Différentes technologies.

- Bo, F., Xianping, L., Jinqing, W., Pengcheng, W., 2015a. The flotation separation of scheelite from calcite using acidified sodium silicate as depressant. *Minerals Engineering* 80, 45–49. <https://doi.org/10.1016/j.mineng.2015.06.017>
- Bo, F., Xianping, L., Jinqing, W., Pengcheng, W., 2015b. The flotation separation of scheelite from calcite using acidified sodium silicate as depressant. *Minerals Engineering* 80, 45–49. <https://doi.org/10.1016/j.mineng.2015.06.017>
- Burt, R., 1999. The role of gravity concentration in modern processing plants. *Minerals Engineering* 12, 1291–1300.
- Chen, W., Feng, Q., Zhang, G., Yang, Q., Zhang, C., 2017. The effect of sodium alginate on the flotation separation of scheelite from calcite and fluorite. *Minerals Engineering* 113, 1–7. <https://doi.org/10.1016/j.mineng.2017.07.016>
- Das, A., Sarkar, B., 2018. Advanced Gravity Concentration of Fine Particles: A Review. *Mineral Processing and Extractive Metallurgy Review* 39, 359–394. <https://doi.org/10.1080/08827508.2018.1433176>
- Dawson, K.M., 1995. Skarn tungsten (No. 8). <https://doi.org/10.4095/208024>
- Dehaine, Q., Filippov, L.O., Glass, H.J., Rollinson, G., 2019a. Rare-metal granites as a potential source of critical metals: A geometallurgical case study. *Ore Geology Reviews* 104, 384–402. <https://doi.org/10.1016/j.oregeorev.2018.11.012>
- Dehaine, Q., Foucaud, Y., Kroll-Rabotin, J.-S., Filippov, L.O., 2019b. Experimental investigation into the kinetics of Falcon UF concentration: Implications for fluid dynamic-based modelling. *Separation and Purification Technology*. <https://doi.org/10.1016/j.seppur.2019.01.048>
- Deng, L., Zhao, G., Zhong, H., Wang, S., Liu, G., 2016. Investigation on the selectivity of N-((hydroxyamino)-alkyl) alkylamide surfactants for scheelite/calcite flotation separation. *Journal of Industrial and Engineering Chemistry* 33, 131–141. <https://doi.org/10.1016/j.jiec.2015.09.027>
- Dias, R., Ribeiro, A., Coke, C., Moreira, N., Romão, J., 2014. Arco Ibero-Armoricano: indentação versus auto-subducção Ibero-Armorican Arc: indentation versus self-subduction 4.

- European Commission, 2010. Critical raw materials for the EU: Report of the Ad-hoc Working Group on defining critical raw materials.
- Falconer, A., 2003. Gravity Separation: Old Technique/New Methods. *Physical Separation in Science and Engineering* 12, 31–48. <https://doi.org/10.1080/1478647031000104293>
- Feng, B., Guo, W., Xu, H., Peng, J., Luo, X., Zhu, X., 2017. The combined effect of lead ion and sodium silicate in the flotation separation of scheelite from calcite. *Separation Science and Technology* 52, 567–573. <https://doi.org/10.1080/01496395.2016.1260590>
- Filippov, L.O., Dehaine, Q., Filippova, I.V., 2016. Rare earths (La, Ce, Nd) and rare metals (Sn, Nb, W) as by-products of kaolin production – Part 3: Processing of fines using gravity and flotation. *Minerals Engineering* 95, 96–106. <https://doi.org/10.1016/j.mineng.2016.06.004>
- Filippov, L.O., Foucaud, Y., Filippova, I.V., Badawi, M., 2018. New reagent formulations for selective flotation of scheelite from a skarn ore with complex calcium minerals gangue. *Minerals Engineering* 123, 85–94. <https://doi.org/10.1016/j.mineng.2018.05.001>
- Filippova, I.V., Filippov, L.O., Duverger, A., Severov, V.V., 2014. Synergetic effect of a mixture of anionic and nonionic reagents: Ca mineral contrast separation by flotation at neutral pH. *Minerals Engineering* 66–68, 135–144. <https://doi.org/10.1016/j.mineng.2014.05.009>
- Foucaud, Y., Dehaine, Q., Filippov, L.O., Filippova, I.V., 2019a. Application of Falcon Centrifuge as a Cleaner Alternative for Complex Tungsten Ore Processing. *Minerals* 9, 448. <https://doi.org/10.3390/min9070448>
- Foucaud, Y., Filippova, I.V., Filippov, L.O., 2019b. Investigation of the depressants involved in the selective flotation of scheelite from apatite, fluorite, and calcium silicates: Focus on the sodium silicate/sodium carbonate system. *Powder Technology* 352, 501–512. <https://doi.org/10.1016/j.powtec.2019.04.071>
- Foucaud, Y., Lebègue, S., Filippov, L.O., Filippova, I.V., Badawi, M., 2018a. Molecular Insight into Fatty Acid Adsorption on Bare and Hydrated (111) Fluorite Surface. *The Journal of Physical Chemistry B* 122, 12403–12410. <https://doi.org/10.1021/acs.jpcc.8b08969>
- Foucaud, Y., Lechenard, B., Marion, P., Filippova, I., Filippov, L., 2018b. Geology, Textural Study, Ore Genesis and Processing of the Tabuaço Tungsten Deposit (Northern Portugal), in: *Al-*

- Juboury, A.I. (Ed.), Contributions to Mineralization. InTech.
<https://doi.org/10.5772/intechopen.71674>
- Gao, Z., Bai, D., Sun, W., Cao, X., Hu, Y., 2015. Selective flotation of scheelite from calcite and fluorite using a collector mixture. *Minerals Engineering* 72, 23–26.
<https://doi.org/10.1016/j.mineng.2014.12.025>
- Hiçyılmaz, C., Atalay, ü., Özbayoglu, G., 1993. Selective flotation of scheelite using amines. *Minerals Engineering* 6, 313–320. [https://doi.org/10.1016/0892-6875\(93\)90039-P](https://doi.org/10.1016/0892-6875(93)90039-P)
- Jébrak, M., Marcoux, É., Laithier, M., 2016. *Geology of mineral resources*, Second edition. ed. Geological Association of Canada, St. John's, NL.
- Kupka, N., Rudolph, M., 2018. Froth flotation of scheelite – A review. *International Journal of Mining Science and Technology* 28, 373–384. <https://doi.org/10.1016/j.ijmst.2017.12.001>
- Liu, C., Feng, Q., Zhang, G., Chen, W., Chen, Y., 2016. Effect of depressants in the selective flotation of scheelite and calcite using oxidized paraffin soap as collector. *International Journal of Mineral Processing* 157, 210–215. <https://doi.org/10.1016/j.minpro.2016.11.011>
- Liu, X., Luo, H., Cheng, R., Li, C., Zhang, J., 2017. Effect of citric acid and flotation performance of combined depressant on collophanite ore. *Minerals Engineering* 109, 162–168.
<https://doi.org/10.1016/j.mineng.2017.03.010>
- Marinakos, K. I., Shergold, H.L., 1985. The mechanism of fatty acid adsorption in the presence of fluorite, calcite and barite. *International journal of mineral processing* 14, 161–176.
- Marinakos, K.I., Shergold, H.L., 1985. Influence of sodium silicate addition on the adsorption of oleic acid by fluorite, calcite and barite. *International Journal of Mineral Processing* 14, 177–193.
[https://doi.org/10.1016/0301-7516\(85\)90002-X](https://doi.org/10.1016/0301-7516(85)90002-X)
- Miller, J.D., Misra, M., 1984. The Hydrophobic Character of Semisoluble Salt Minerals with Oleate as Collector. *International Conference on Recent Advances in Mineral Sciences and Technologic*, Johannesburg, South Africa 259–267.
- Pastor, H., 2000. *Métallurgie et recyclage du tungstène*. Procédés.
- Pinto, M.D., Ribeiro, M.A., Noronha, F., 2016. Rochas calcossilicatadas e metagrauwaques da Formação de Bateiras (CXG – Grupo do Douro) 5.

- Pitfield, P., Brown, T., Gunn, G., Rayner, D., 2011. Tungsten profile. London: British Geological Survey [Online], 2011. <https://www.bgs.ac.uk/downloads/start.cfm?id=1981>.
- Pugh, R., Stenius, P., 1985. Solution chemistry studies and flotation behaviour of apatite, calcite and fluorite minerals with sodium oleate collector. *International journal of mineral processing* 15, 193–218.
- Rao, K.H., Antti, B.-M., Forssberg, E., 1988. Mechanism of oleate interaction on salt-type minerals part I. Adsorption and electrokinetic studies of calcite in the presence of sodium oleate and sodium metasilicate. *Colloids and Surfaces* 34, 227–239. [https://doi.org/10.1016/0166-6622\(88\)80101-X](https://doi.org/10.1016/0166-6622(88)80101-X)
- Tomas, H., 1985. Le traitement des minerais de tungstène à Salau.
- Wang, Y., Yu, F., 2007. Effects of Metallic Ions on the Flotation of Spodumene and Beryl. *Journal of China University of Mining and Technology* 17, 35–39. [https://doi.org/10.1016/S1006-1266\(07\)60008-X](https://doi.org/10.1016/S1006-1266(07)60008-X)
- Wells, A., 1991. Some experiences in the design and optimisation of fine gravity concentration circuits. *Minerals Engineering* 4, 383–398. [https://doi.org/10.1016/0892-6875\(91\)90143-J](https://doi.org/10.1016/0892-6875(91)90143-J)
- Yang, X., 2018. Beneficiation studies of tungsten ores – A review. *Minerals Engineering* 125, 111–119. <https://doi.org/10.1016/j.mineng.2018.06.001>
- Yang, Y., Xie, B., Wang, R., Xu, S., Wang, J., Xu, Z., 2016. Extraction and separation of tungsten from acidic high-phosphorus solution. *Hydrometallurgy* 164, 97–102. <https://doi.org/10.1016/j.hydromet.2016.05.018>
- Yongxin, L., Changgen, L., 1983a. Selective flotation of scheelite from calcium minerals with sodium oleate as a collector and phosphates as modifiers. I. Selective flotation of scheelite. *International Journal of Mineral Processing* 10, 205–218. [https://doi.org/10.1016/0301-7516\(83\)90011-X](https://doi.org/10.1016/0301-7516(83)90011-X)
- Yongxin, L., Changgen, L., 1983b. Selective flotation of scheelite from calcium minerals with sodium oleate as a collector and phosphates as modifiers. I. Selective flotation of scheelite. *International Journal of Mineral Processing* 10, 205–218. [https://doi.org/10.1016/0301-7516\(83\)90011-X](https://doi.org/10.1016/0301-7516(83)90011-X)

- Zhang, Y., Li, Y., Chen, R., Wang, Y., Deng, J., Luo, X., 2017. Flotation Separation of Scheelite from Fluorite Using Sodium Polyacrylate as Inhibitor. *Minerals* 7, 102. <https://doi.org/10.3390/min7060102>
- Zhao, G., Wang, S., Zhong, H., 2015. Study on the Activation of Scheelite and Wolframite by Lead Nitrate. *Minerals* 5, 247–258. <https://doi.org/10.3390/min5020247>
- Zhao, G., Zhong, H., Qiu, X., Wang, S., Gao, Y., Dai, Z., Huang, J., Liu, G., 2013. The DFT study of cyclohexyl hydroxamic acid as a collector in scheelite flotation. *Minerals Engineering* 49, 54–60. <https://doi.org/10.1016/j.mineng.2013.04.025>